Supplemental Materials

Effects of age, sex, and extracellular matrix integrity on aortic dilatation and rupture in a mouse model of Marfan syndrome

D. Weiss[1], B.V. Rego[1], C. Cavinato[1], D.S. Li[1], Y. Kawamura[1], N. Emuna[1], J.D Humphrey[1,2]

[1]Department of Biomedical Engineering
Yale University, New Haven, CT

[2]Vascular Biology and Therapeutics Program
Yale School of Medicine, New Haven, CT

Running title: Age, Sex, and ECM Cross-Linking in MFS

Address for Correspondence:

Dar Weiss, Ph.D.
Department of Biomedical Engineering
Yale University, New Haven, CT 06520 USA
dar.weiss@yale.edu
+1-203-508-2118

SUPPLEMENTAL TABLES

Table S1. Quantification of layer-specific cross-sectional areas and microstructural composition of the primary matrix constituents (collagen, elastin, cytoplasm and GAGs) from all 8 of the 4-8 week groups, evaluated at 8 weeks of age (mean ± standard deviation).

	4-8 Week Groups (evaluations at 8 weeks of age)							
	Controls				BAPN			
	MWT n = 6	FWT n = 6	MMFS n = 5	FMFS n = 6	MWT n = 6	FWT n = 7	MMFS n = 8	FMFS n = 8
Wall Area ($x10^{-3}mm^2$)								
Total	58.84 ± 0.88	64.54 ± 6.46	57.84 ± 6.87	59.45 ± 8.84	63.07 ± 15.08	109.12 ± 28.53	201.78 ± 94.61	86.01 ± 45.98
Media	41.37 ± 0.17	47.42 ± 4.50	43.74 ± 4.79	45.19 ± 6.32	47.44 ± 11.18	64.16 ± 17.81	92.88 ± 28.65	57.55 ± 25.50
Adventitia	17.47 ± 0.71	17.12 ± 1.96	14.10 ± 2.08	14.26 ± 2.52	15.63 ± 3.90	44.96 ± 10.72	108.90 ± 65.96	28.46 ± 20.48
% Media	70.31	73.47	75.62	76.01	75.22	58.80	46.03	66.91
% Adventitia	29.69	26.53	24.38	23.99	24.78	41.20	53.97	33.09
MOVAT (Area Fraction)								
medial-GAGs	0.0674 ± 0.0041	0.0361 ± 0.0062	0.1027 ± 0.0072	0.0845 ± 0.0083	0.1052 ± 0.0085	0.1093 ± 0.0067	0.0997 ± 0.0036	0.1295 ± 0.0095
medial-Collagen	0.2147 ± 0.0082	0.1901 ± 0.0167	0.1979 ± 0.0120	0.1823 ± 0.0175	0.1229 ± 0.0064	0.1565 ± 0.0165	0.1468 ± 0.0102	0.1093 ± 0.0123
medial-Cytoplasm	0.1073 ± 0.0060	0.1424 ± 0.0038	0.0887 ± 0.0037	0.1387 ± 0.0037	0.0875 ± 0.0059	0.0698 ± 0.0023	0.0561 ± 0.0062	0.0915 ± 0.0050
medial-Elastin	0.3010 ± 0.0117	0.3314 ± 0.0175	0.3477 ± 0.0113	0.3424 ± 0.0180	0.4265 ± 0.0143	0.2387 ± 0.0155	0.1737 ± 0.0149	0.3561 ± 0.0272
Adventitial-GAGs	0.0124 ± 0.0000	0.0109 ± 0.0011	0.0109 ± 0.0011	0.0070 ± 0.0009	0.0058 ± 0.0007	0.0318 ± 0.0055	0.0232 ± 0.0043	0.0169 ± 0.0027
Adventitial-Collagen	0.2667 ± 0.0079	0.2358 ± 0.0057	0.2189 ± 0.0125	0.2172 ± 0.0047	0.2107 ± 0.0056	0.3204 ± 0.0171	0.4101 ± 0.0201	0.2345 ± 0.0062
Adventitial-Cytoplasm	0.0144 ± 0.0008	0.0136 ± 0.0009	0.0088 ± 0.0005	0.0118 ± 0.0011	0.0239 ± 0.0036	0.0538 ± 0.0052	0.0697 ± 0.0051	0.0435 ± 0.0058
Adventitial-Elastin	0.0010 ± 0.0002	0.0010 ± 0.0002	0.0010 ± 0.0001	0.0011 ± 0.0001	0.0015 ± 0.0002	0.0039 ± 0.0006	0.0050 ± 0.0014	0.0041 ± 0.0008
PSR (Area Fraction)								
Thin Collagen Fibers	0.051 ± 0.001	0.053 ± 0.007	0.051 ± 0.005	0.056 ± 0.007	0.037 ± 0.004	0.038 ± 0.006	0.024 ± 0.001	0.024 ± 0.002
Thick Collagen Fibers	0.896 ± 0.003	0.888 ± 0.006	0.905 ± 0.000	0.902 ± 0.008	0.923 ± 0.005	0.928 ± 0.007	0.945 ± 0.001	0.945 ± 0.003

Table S2. Similar to Table S2, except quantification of layer-specific cross-sectional areas and microstructural composition of the primary matrix constituents from all 8 of the 8-12 week groups, evaluated at 12 weeks of age (mean ± standard deviation).

	8-12 Week Groups (evaluations at 12 weeks of age)							
	Controls				BAPN			
	MWT n = 8	FWT n = 7	MMFS n = 7	FMFS n = 8	MWT n = 7	FWT n = 7	MMFS n = 8	FMFS n = 9
Wall Area ($x10^{-3}mm^2$)								
Total	66.77 ± 0.87	65.69 ± 5.16	79.84 ± 7.13	61.68 ± 2.22	57.22 ± 1.14	54.52 ± 5.73	84.45 ± 32.12	86.76 ± 25.82
Media	48.72 ± 0.32	51.43 ± 3.03	54.69 ± 1.84	44.90 ± 0.50	36.54 ± 0.09	42.58 ± 4.98	57.85 ± 14.84	57.19 ± 9.09
Adventitia	18.05 ± 0.55	14.26 ± 2.13	25.15 ± 5.29	16.78 ± 1.72	20.68 ± 1.05	11.94 ± 0.75	26.60 ± 17.28	29.57 ± 16.73
% Media	72.97	78.29	68.50	72.80	63.86	78.10	68.50	65.92
% Adventitia	27.03	21.71	31.50	27.20	36.14	21.90	31.50	34.08
MOVAT (Area Fraction)								
medial-GAGs	0.0996 ± 0.0072	0.1222 ± 0.0059	0.2050 ± 0.0102	0.1165 ± 0.0048	0.0874 ± 0.0034	0.1460 ± 0.0051	0.1437 ± 0.0038	0.1644 ± 0.0147
medial-Collagen	0.3180 ± 0.0051	0.1913 ± 0.0243	0.1814 ± 0.0292	0.1174 ± 0.0065	0.1586 ± 0.0020	0.1975 ± 0.0389	0.2590 ± 0.0042	0.1519 ± 0.0123
medial-Cytoplasm	0.1442 ± 0.0111	0.1523 ± 0.0064	0.2302 ± 0.0172	0.1919 ± 0.0110	0.1436 ± 0.0081	0.1028 ± 0.0167	0.1352 ± 0.0118	0.1660 ± 0.0143
medial-Elastin	0.4242 ± 0.0080	0.5236 ± 0.0282	0.3696 ± 0.0168	0.5589 ± 0.0217	0.5862 ± 0.0089	0.5336 ± 0.0281	0.4457 ± 0.0133	0.5002 ± 0.0226
Adventitial-GAGs	0.0367 ± 0.0013	0.0575 ± 0.0055	0.0661 ± 0.0170	0.0652 ± 0.0010	0.0386 ± 0.0015	0.0234 ± 0.0018	0.0206 ± 0.0009	0.0838 ± 0.0182
Adventitial-Collagen	0.9267 ± 0.0006	0.8680 ± 0.0101	0.8134 ± 0.0532	0.8447 ± 0.0032	0.9214 ± 0.0037	0.8956 ± 0.0156	0.7813 ± 0.0312	0.0507 ± 0.0299
Adventitial-Cytoplasm	0.0240 ± 0.0034	0.0537 ± 0.0058	0.1081 ± 0.0355	0.0701 ± 0.0028	0.0227 ± 0.0018	0.0614 ± 0.0193	0.1831 ± 0.0312	0.1220 ± 0.0116
Adventitial-Elastin	0.0038 ± 0.0007	0.0092 ± 0.0011	0.0054 ± 0.0010	0.0064 ± 0.0004	0.0037 ± 0.0006	0.0060 ± 0.0005	0.0054 ± 0.0008	0.0126 ± 0.0024
PSR (Area Fraction)								
Thin Collagen Fibers	0.051 ± 0.002	0.055 ± 0.004	0.032 ± 0.009	0.086 ± 0.004	0.045 ± 0.013	0.042 ± 0.003	0.015 ± 0.002	0.027 ± 0.004
Thick Collagen Fibers	0.899 ± 0.002	0.895 ± 0.005	0.923 ± 0.011	0.861 ± 0.005	0.914 ± 0.016	0.915 ± 0.004	0.953 ± 0.003	0.941 ± 0.004

Table S3. Key geometric and mechanical metrics (mean ± standard deviation) from all 8 of the 4-8 week groups, evaluated at 8 weeks, including those mice without and with preceding 4-weeks of BAPN. The pressure-dependent quantities were evaluated at a common pressure of 100 mmHg given the lack of a measured differences in tail-cuff blood pressures. Values of stress, stiffness, and stored energy were computed from a single set of material parameters based on over 2800 measurements per specimen that covered a broad range of distending pressures and axial forces.

	4-8 Week Groups (evaluations at 8 weeks of age)							
	No treatment				**BAPN-exposed**			
	MWT	**FWT**	**MMFS**	**FMFS**	**MWT**	**FWT**	**MMFS**	**FMFS**
	n = 5	**n = 5**	**n = 5**	**n = 5**	**n = 5**	**n = 5**	**n = 5**	**n = 5**
Unloaded dimensions								
Wall Thickness (μm)	125 ± 8	141 ± 13	123 ± 7	129 ± 8	129 ± 6	125 ± 5	257 ± 43	189 ± 23
Outer Diameter (μm)	1103 ± 29	1131 ± 9	1216 ± 33	1173 ± 21	945 ± 35	1013 ± 29	1784 ± 268	1289 ± 134
Loaded dimensions	**P=100 mmHg**							
Outer Diameter (μm)	1738 ± 42	1760 ± 36	1908 ± 64	1788 ± 33	1553 ± 37	1532 ± 49	2684 ± 288	1907 ± 160
Wall Thickness (μm)	42 ± 3	49 ± 5	41 ± 2	45 ± 3	42 ± 4	48 ± 3	123 ± 29	85 ± 14
Inner Radius (μm)	827 ± 22	831 ± 19	913 ± 32	849 ± 16	735 ± 19	718 ± 25	1219 ± 144	869 ± 80
in vivo Axial Stretch (λ_z^{iv})	1.72 ± 0.04	1.67 ± 0.04	1.63 ± 0.04	1.69 ± 0.03	1.68 ± 0.04	1.57 ± 0.06	1.32 ± 0.10	1.38 ± 0.09
in vivo Circumferential Stretch (λ_ϑ)	1.73 ± 0.02	1.73 ± 0.04	1.69 ± 0.03	1.67 ± 0.01	1.86 ± 0.06	1.67 ± 0.04	1.73 ± 0.08	1.68 ± 0.07
Cauchy Stresses (kPa)								
Circumferential, σ_ϑ	267 ± 16	238 ± 31	283 ± 17	253 ± 14	229 ± 16	204 ± 17	156 ± 26	150 ± 22
Axial, σ_z	236 ± 18	203 ± 25	235 ± 12	208 ± 11	216 ± 18	167 ± 17	88 ± 24	107 ± 22
Linearized Stiffness (MPa)								
Circumferential, C_{qqqq}	1.56 ± 0.11	1.45 ± 0.22	3.04 ± 0.28	2.53 ± 0.16	1.43 ± 0.18	1.41 ± 0.15	2.27 ± 0.59	2.98 ± 0.39
Axial, C_{zzzz}	1.10 ± 0.07	0.94 ± 0.11	1.33 ± 0.07	1.15 ± 0.07	1.20 ± 0.08	0.93 ± 0.07	0.47 ± 0.11	0.83 ± 0.10
Stored Energy (kPa)	82 ± 3	72 ± 6	63 ± 4	55 ± 3	62 ± 4	49 ± 6	22 ± 6	21 ± 5

Table S4. Similar to Table S3 except for the 8 groups of mice evaluated at 12 weeks of age without and with preceding 4-weeks of BAPN.

	8-12 Week Groups (evaluations at 12 weeks of age)							
	No treatment				BAPN-exposed			
	MWT n = 5	FWT n =5	MMFS n =5	FMFS n =5	MWT n =5	FWT n =5	MMFS n =5	FMFS n = 5
Unloaded dimensions								
Wall Thickness (μm)	135 ± 6	132 ± 6	144 ± 18	140 ± 7	129 ± 2	113 ± 3	183 ± 20	164 ± 15
Outer Diameter (μm)	1098 ± 88	1144 ± 24	1320 ± 146	1094 ± 42	1022 ± 40	1022 ± 38	1470 ± 174	1215 ± 113
Loaded dimensions				P=100 mmHg				
Outer Diameter (μm)	1756 ± 24	1718 ± 16	1918 ± 141	1740 ± 28	1679 ± 42	1625 ± 93	2130 ± 168	1946 ± 195
Wall Thickness (μm)	48 ± 2	47 ± 4	58 ± 2	49 ± 3	41 ± 1	40 ± 2	82 ± 17	63 ± 8
Inner Radius (μm)	830 ± 22	812 ± 19	901 ± 32	821 ± 16	799 ± 19	773 ± 25	983 ± 144	910 ± 80
in vivo Axial Stretch (λ_z^{iv})	1.77 ± 0.03	1.70 ± 0.04	1.56 ± 0.05	1.64 ± 0.02	1.71 ± 0.04	1.64 ± 0.06	1.48 ± 0.08	1.48 ± 0.07
in vivo Circumferential Stretch (λ_ϑ)	1.69 ± 0.02	1.67 ± 0.01	1.60 ± 0.10	1.74 ± 0.05	1.84 ± 0.05	1.73 ± 0.04	1.63 ± 0.08	1.79 ± 0.03
Cauchy Stresses (kPa)								
Circumferential, σ_ϑ	205 ± 34	240 ± 19	209 ± 23	215 ± 17	262 ± 5	263 ± 28	179 ± 22	196 ± 9
Axial, σ_z	204 ± 2	220 ± 16	156 ± 15	185 ± 12	244 ± 12	234 ± 20	128 ± 23	156 ± 19
Linearized Stiffness (MPa)								
Circumferential, $C_{\vartheta\vartheta\vartheta\vartheta}$	1.38 ± 0.06	1.50 ± 0.12	2.84 ± 0.62	2.13 ± 0.09	1.58 ± 0.08	1.62 ± 0.19	3.11 ± 0.43	2.37 ± 0.26
Axial, C_{zzzz}	1.07 ± 0.02	1.06 ± 0.07	1.05 ± 0.21	1.05 ± 0.05	1.22 ± 0.06	1.25 ± 0.06	0.86 ± 0.14	0.98 ± 0.09
Stored Energy (kPa)	71 ± 7	70 ± 3	37 ± 1	48 ± 4	74 ± 3	65 ± 6	29 ± 7	35 ± 5

SUPPLEMENTAL FIGURES

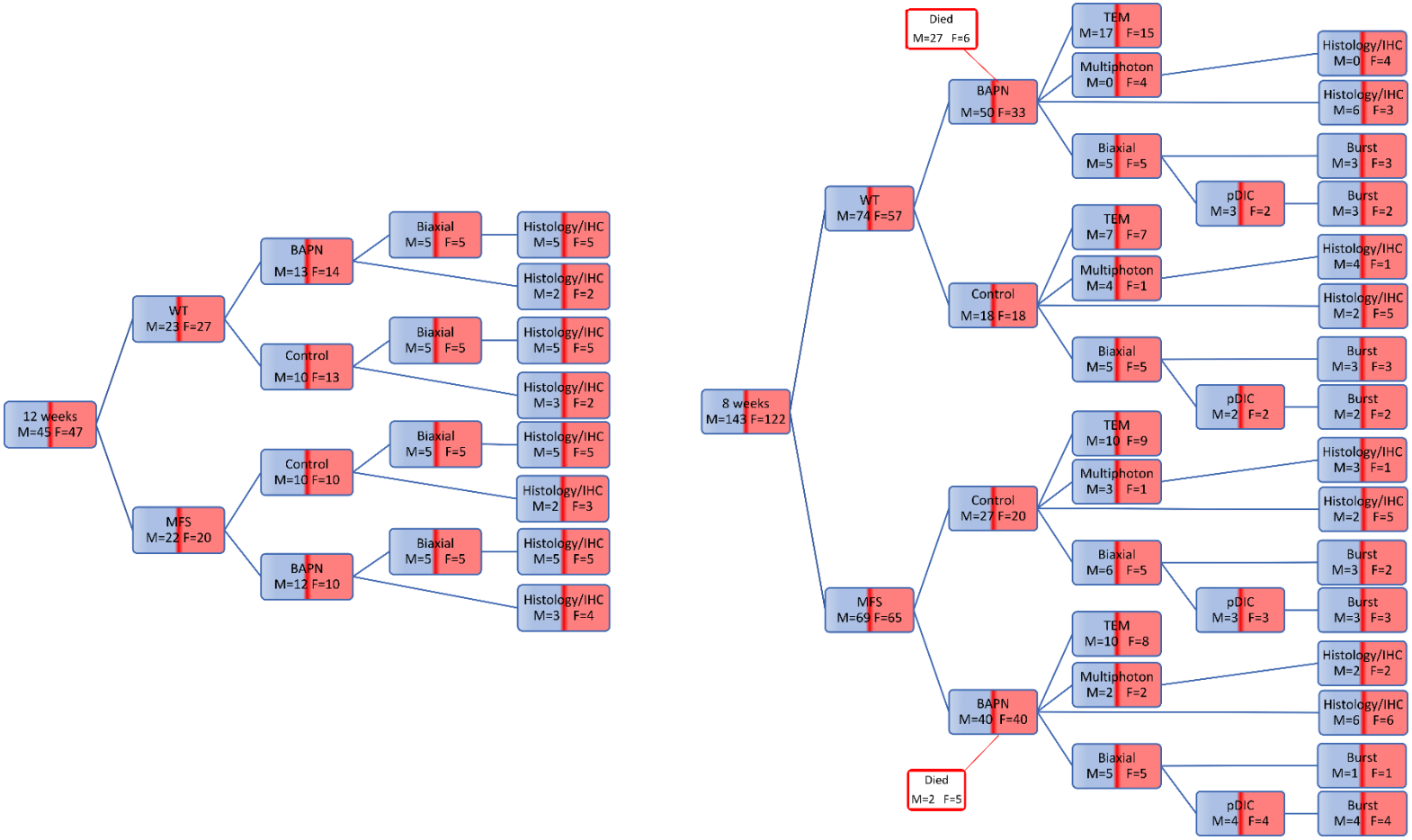

Figure S1 – Overall study design. Distributed use of *n* = 357 mice: 45 males (M – light blue) and 47 females (F – light red) at 12 weeks of age (left) plus 143 males and 122 females at 8 weeks of age (right). Of these, 181 were wild-type (*Fbn1*$^{+/+}$ WT) and 176 were Marfan (*Fbn1*$^{C1041G/+}$ MFS) mice. Note the four primary uses: standard biaxial testing, standard histology and immuno-histochemistry, transmission electron microscopy, and pressure-burst testing for which each group consisted of 5 or more (5-17) samples. More mice were studied at 8 than 12 weeks of age given the hypothesis and early observation of a more severe phenotype in younger mice. Note, too, that additional data were collected for the younger mice, including panoramic digital imaging correlation (pDIC, to confirm and extend biaxial data) and multiphoton microscopy (to confirm and extend histological data).

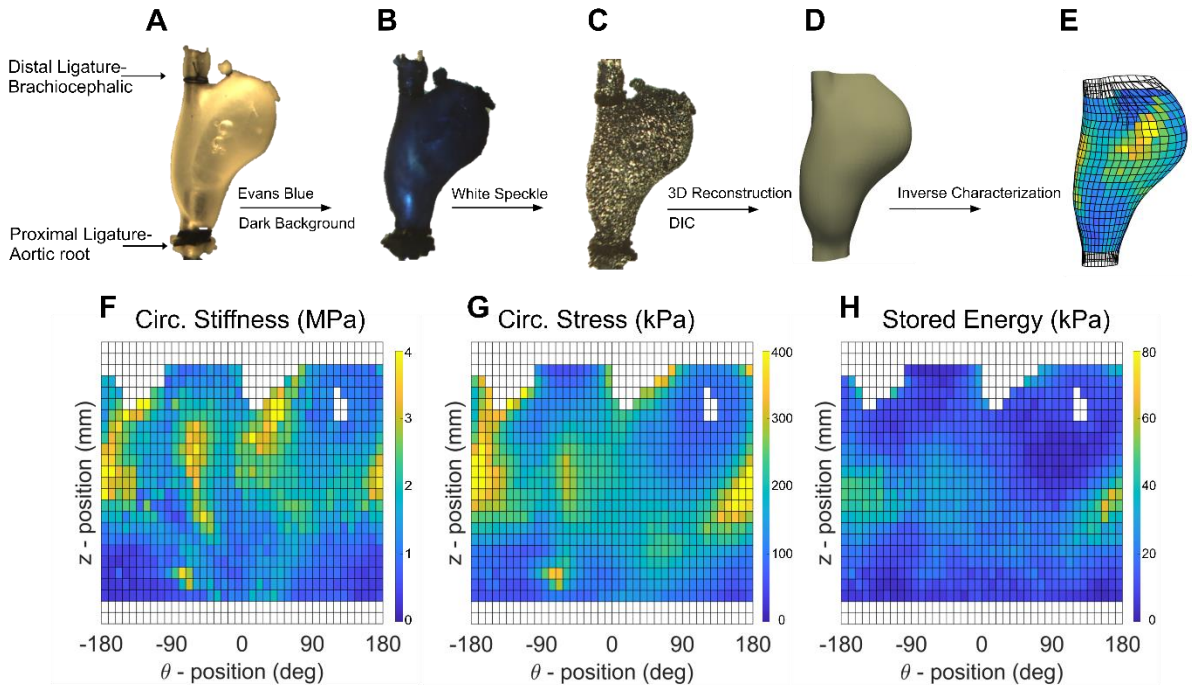

Figure S2 – pDIC method. Regional material characterization. Following standard biaxial testing, aortas from a subset of the 8-week old mice were re-cannulated and secured on a triple blunt-end needle assembly (A), soaked in Evans blue dye to create a dark background (B), and then air-brushed with a white India ink to form a unique speckle pattern on the vessel surface (C). The vessel was then submerged in a HBSS-filled 45-degree conical mirror and the reflection of the white pattern was captured by a nearly vertically located digital camera from 8 different rotationally symmetric views at 14 incremental pressures (10-140, 10 mmHg increments) and 3 axial stretches (λ_z^{iv} and ±5% of this value) for 336 images per vessel (over 42 loading states). Digital image correlations over all deformed configurations were then used to reconstruct the 3D surface geometry (D) at each deformed configuration and to compute full-field surface deformations that were used to estimate best-fit parameters for our four-fiber constitutive relation locally at ~1000 elements around the circumference (θ position) and along the length (Z position) of each specimen. The principle of virtual power was enforced at each element to achieve inverse characterization (i.e., parameter estimation) and to compute full-field distributions of the mechanical metrics, including circumferential stiffness (E, F- unwrapped 2D map), circumferential stress (G), and stored energy (H).

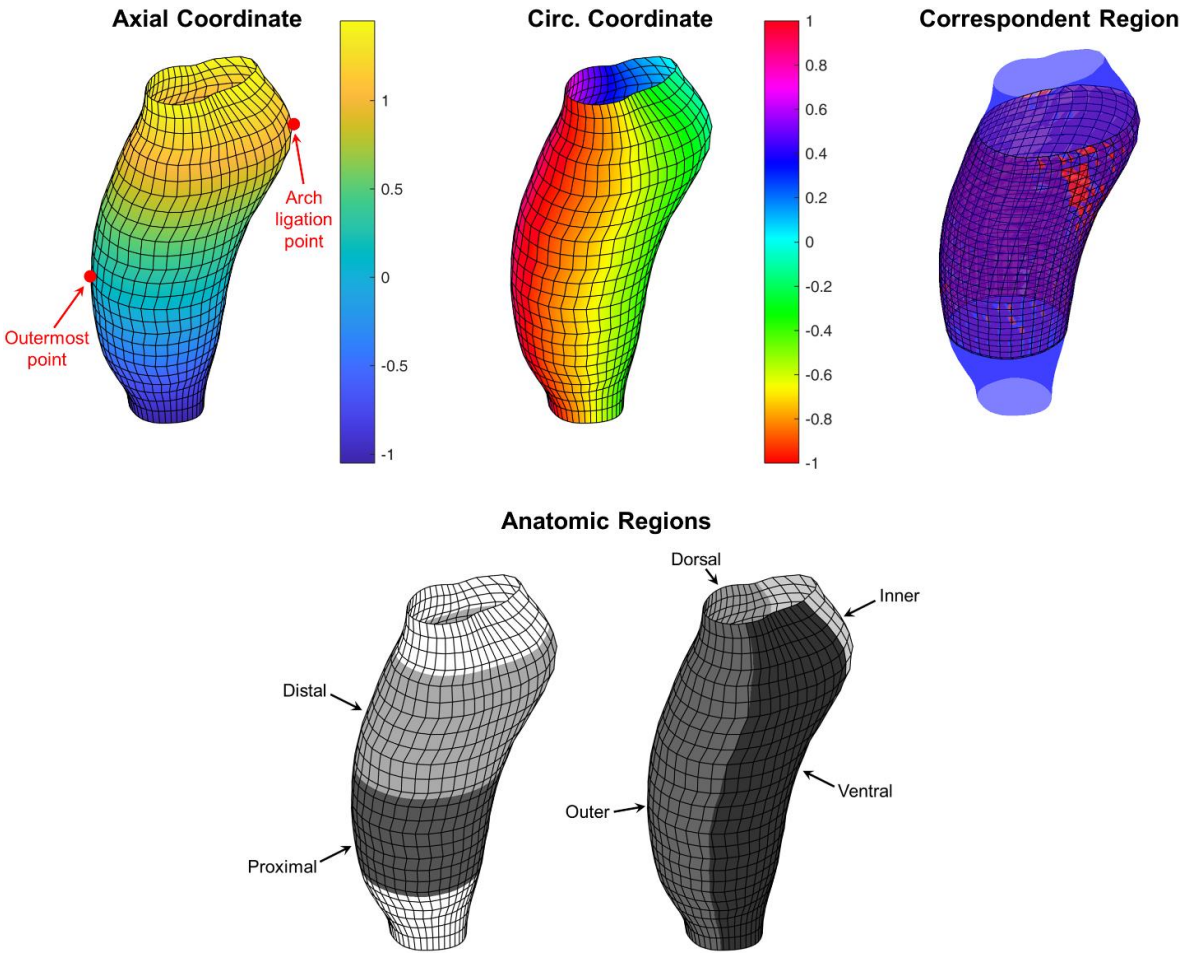

Figure S3 – pDIC method. Pipeline for geometric parametrization and subsequent co-registration of pDIC-based and OCT-based three-dimensional geometries, shown here for a representative normal MWT ascending aorta. Along the axial direction, the vessel is parametrized using two anatomic landmarks (red points) such that the axial coordinate is 0 at the outermost point on the outer curvature and 1 at the ligature at the distal end (note that parts of the vessel surface lie outside this interval, thus the axial coordinate values extend beyond the [0, 1] interval). Around the circumference, the vessel is parametrized with periodic boundaries at -1 and 1, located in the middle of the outer curvature. Statistical analyses and modeling were performed only within the "correspondent region" that was spanned by all vessel geometries included in the dataset. For interpretation and presentation of the results, the correspondent region was segmented into two regions along the axial direction (proximal and distal) and four regions circumferentially (inner, dorsal, outer, and ventral).

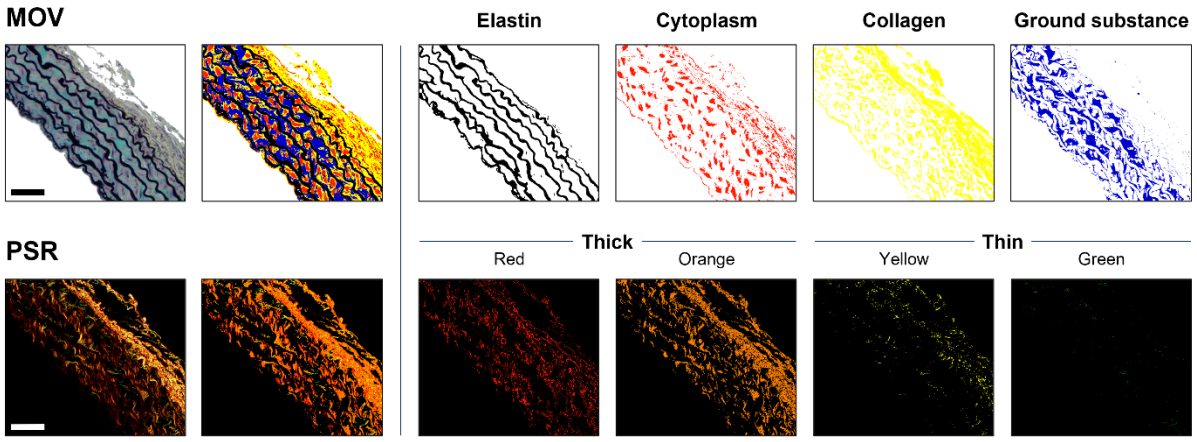

Figure S4 – Quantitative histological method. Representative histological analysis of (top) Movat (MOV)-stained and (bottom) picro-sirius red (PSR)-stained cross-sections. Custom color-based analysis routines were used to categorize image pixels as elastin (black), cytoplasm (red), fibrillar collagen (yellow), ground substance (blue), or fibrin (not shown) in MOV images, and to detect fibrillar collages in a spectrum from red-to-green in PSR images, digitally separated from the analyzed image for clarity. In PSR images, red/orange and yellow/green pixels were categorized as thick and thin fibers, respectively. MOV images were collected under standard bright-field conditions (180 µs exposure) while PSR images were collected under dark-field conditions using polarized light (32 ms exposure). Scale bar = 100 µm. The custom code used for quantification can be found at: https://github.com/yale-cbl/histological-analysis.

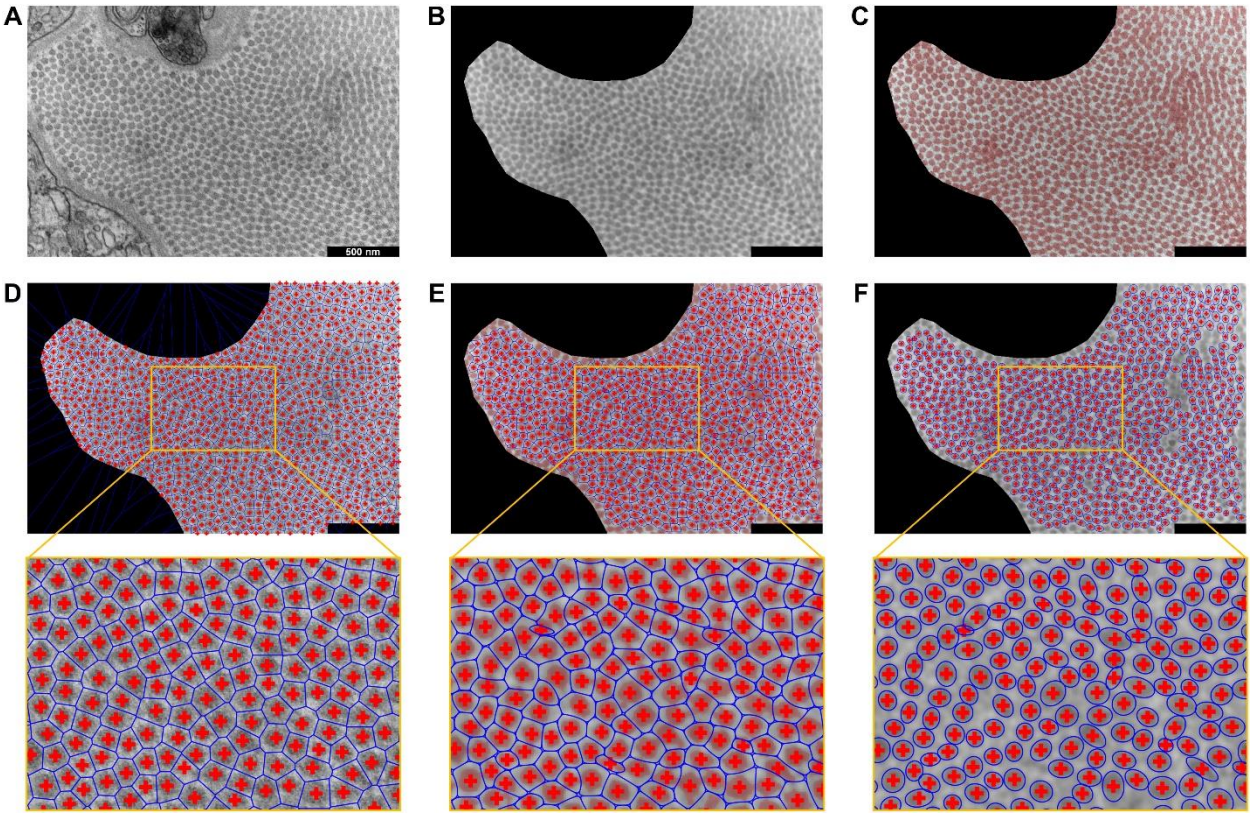

Figure S5 – TEM method. Pipeline for semi-automated processing of TEM images to quantify collagen fibril locations, size, and shape. The original image (A) is interactively edited to exclude regions that do not contain fibrils, smoothed with a Gaussian filter (B), and automatically thresholded as a first attempt to segment fibril and non-fibril pixels (C, with thresholded regions shaded red). Fibril centroid locations (red crosses) are then automatically detected to estimate individual fibril "neighborhoods" as Voronoi cells (D, with neighborhood boundaries shown in blue), which are then interactively corrected by the user if necessary. The user-corrected fibril centroid locations are used to fine-tune the thresholding as a spatially heterogeneous field, and as an initial guess to fit a Gaussian mixture model to the new set of pixels estimated to belong to fibrils (E, where the blue boundary around each fibril neighborhood is the level set at which the membership probability of a thresholded pixel belonging to that fibril equals 50%). Under the approximation that thresholded pixels within a fibril are uniformly distributed within an ellipse, size, orientation, and aspect ratio of the best-fit ellipse are computed automatically (F).

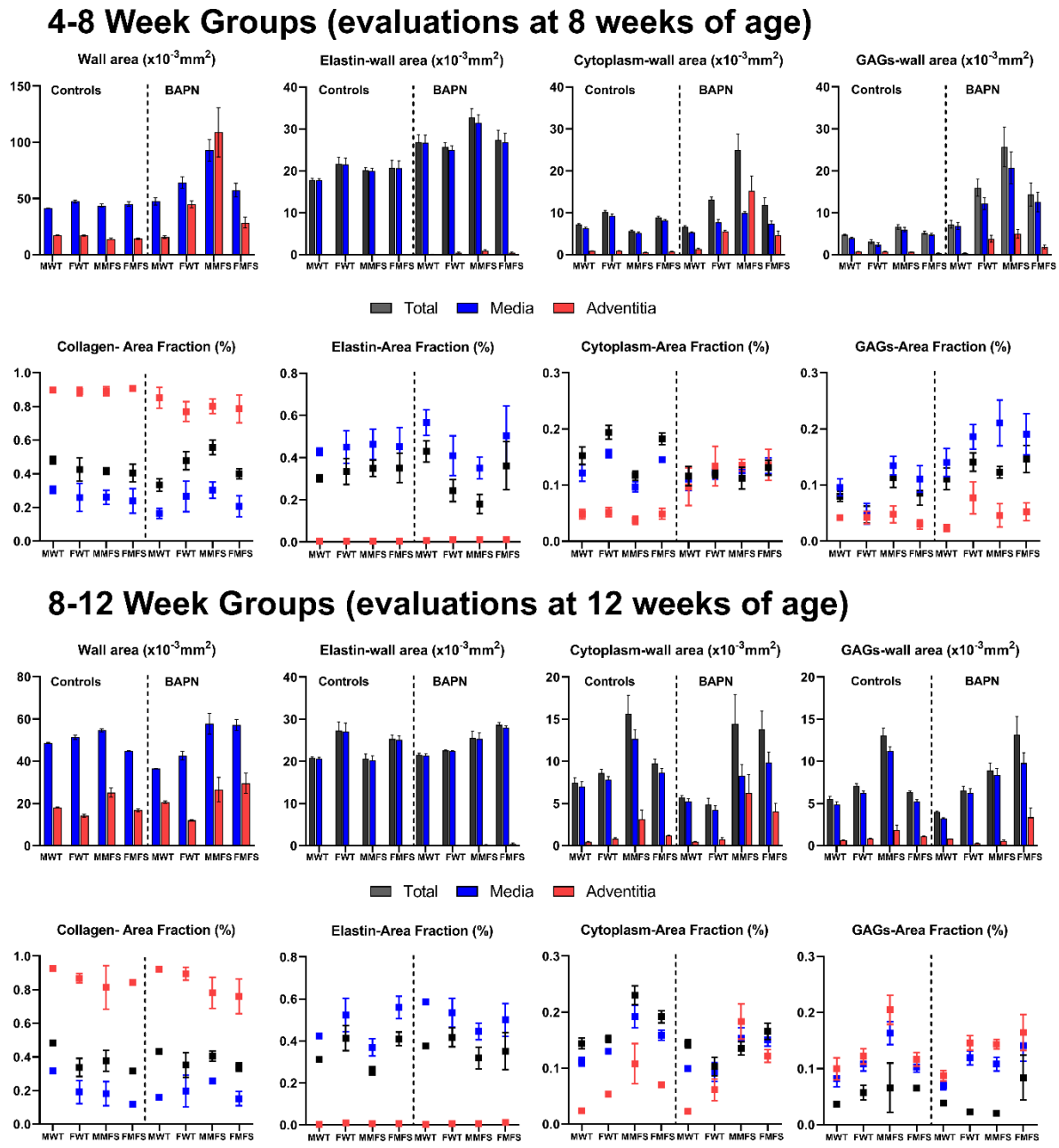

Figure S6 – Quantitative histology for all 16 groups, namely, those evaluated at 8 weeks of age (4-8 week groups) and at 12 weeks of age (8-12 week groups). A companion to Figure 1 in the main text, shown here is additional layer-specific quantification of Movat-stained sections. Data are presented for wall area and area fraction with mean ± standard deviation (*n* = 5-9 sections per group, see Tables S1 and S2). Note the increase of adventitial cytoplasm in the BAPN-exposed 8-week old groups, particularly in male MFS mice, consistent with multiphoton observations (below).

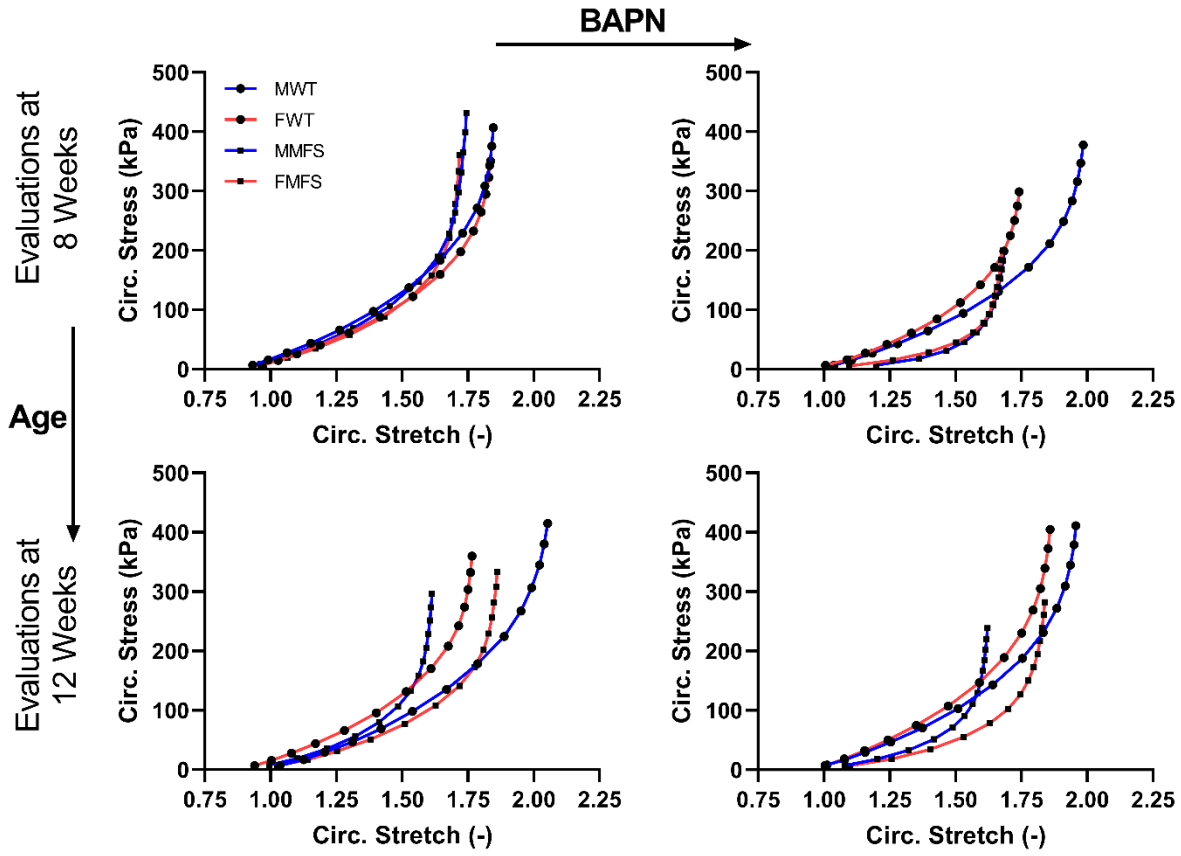

Figure S7 – Stress-stretch data for all 16 groups, namely, those evaluated at 8 and 12 weeks of age. Similar to Figure 2 in the main text, but for circumferential Cauchy stress-stretch behaviors for the ascending aorta for the same 16 groups (n = 5 per group, or 80 samples total). Note that the values shown (solid symbols) represent means for 1 of the 7 cyclic protocols performed (pressurization while held at the *in vivo* value of axial stretch), with a reduced number of data points shown for clarity since each curve is defined by over 100 data points per channel (diameter, length, pressure, force) that are collected on-line by the computer. These results are thus not compared statistically since they show a visually interpretable subset of the full data set, which is quantified and compared in Figures 3 and S8.

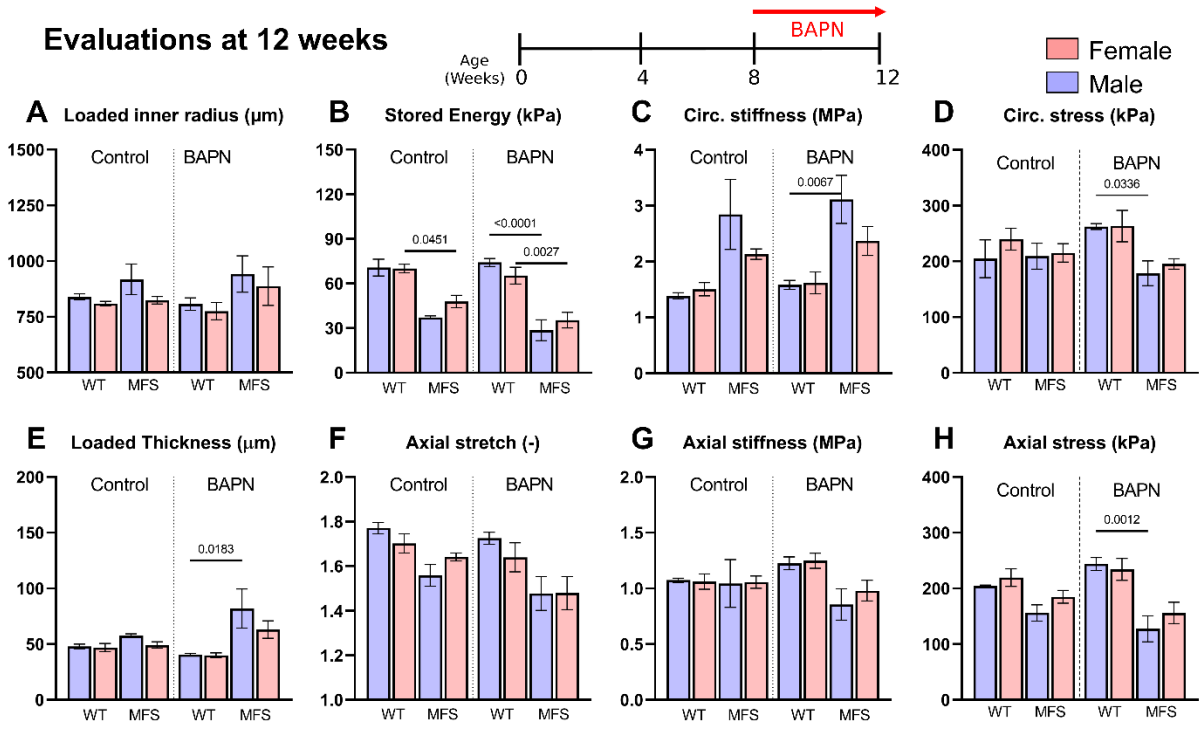

Figure S8 – Biaxial data evaluated at 12 weeks of age (8-12 week groups). Similar to Figure 3 in the main text, but comparing 8 key geometric and mechanical metrics (panels A-H) for female (F, light red) and male (M, light blue), wild-type (WT) and *Fbn1*$^{C1041G/+}$ (MFS) ascending aortas with BAPN given for 4 weeks beginning at 8 weeks of age (then evaluated at 12 weeks), with age- and sex-matched controls not receiving BAPN. These values (mean ± standard deviation) were inferred from *ex vivo* mechanical testing of excised segments (with n=5 per group, 40 aortas tested over the 8 overall groups of older mice) under physiological conditions, with each mechanical metric calculated from biaxial data from 7 cyclic loading protocols that yielded over 2800 data points per cycle for each of the 40 vessels (i.e., these comparisons of mechanical metrics are based on over 112000 on-line computer-controlled measurements). Statistical comparisons by non-parametric Kruskal Wallis test followed by Dunn's post-hoc test for multiple comparisons. See Tables S3 and S4 for all numerical values.

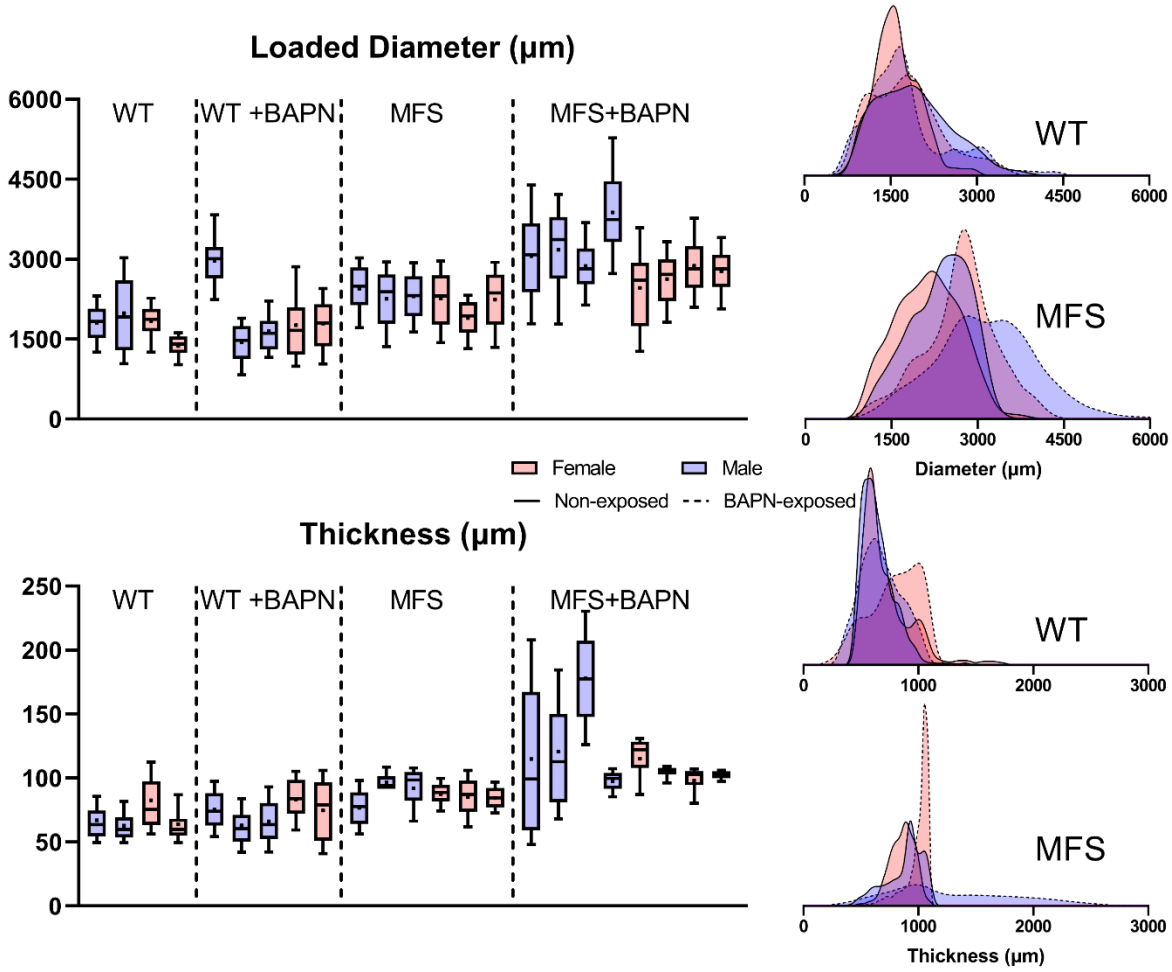

Figure S9 – pDIC data evaluated at 8 weeks of age (4-8 week groups). Locally identified distributions of outer diameter and wall thickness for each of the *n*=23 samples tested with multimodal (see Figure S1) panoramic Digital Image Correlation (pDIC) + optical coherence tomography (OCT), presented as Box-and-Whisker plots (left) and probability density functions (right). See Figure 4 in the main text for values summarized for the 8 groups evaluated at 8 weeks of age. The thickness values were measured using OCT and were collected at 100 cross-sections along the length of each vessel and mapped onto the pDIC reconstructed geometry using an automatic co-registration pipeline. Loaded diameter was computed as twice the Euclidean distance from each point on the wall to the nearest point on the curvilinear centerline of the vessel. Each bar plot represents ~1000 results around the circumference and along the length of each specimen, thus ~23000 data points are represented in each of these plots.

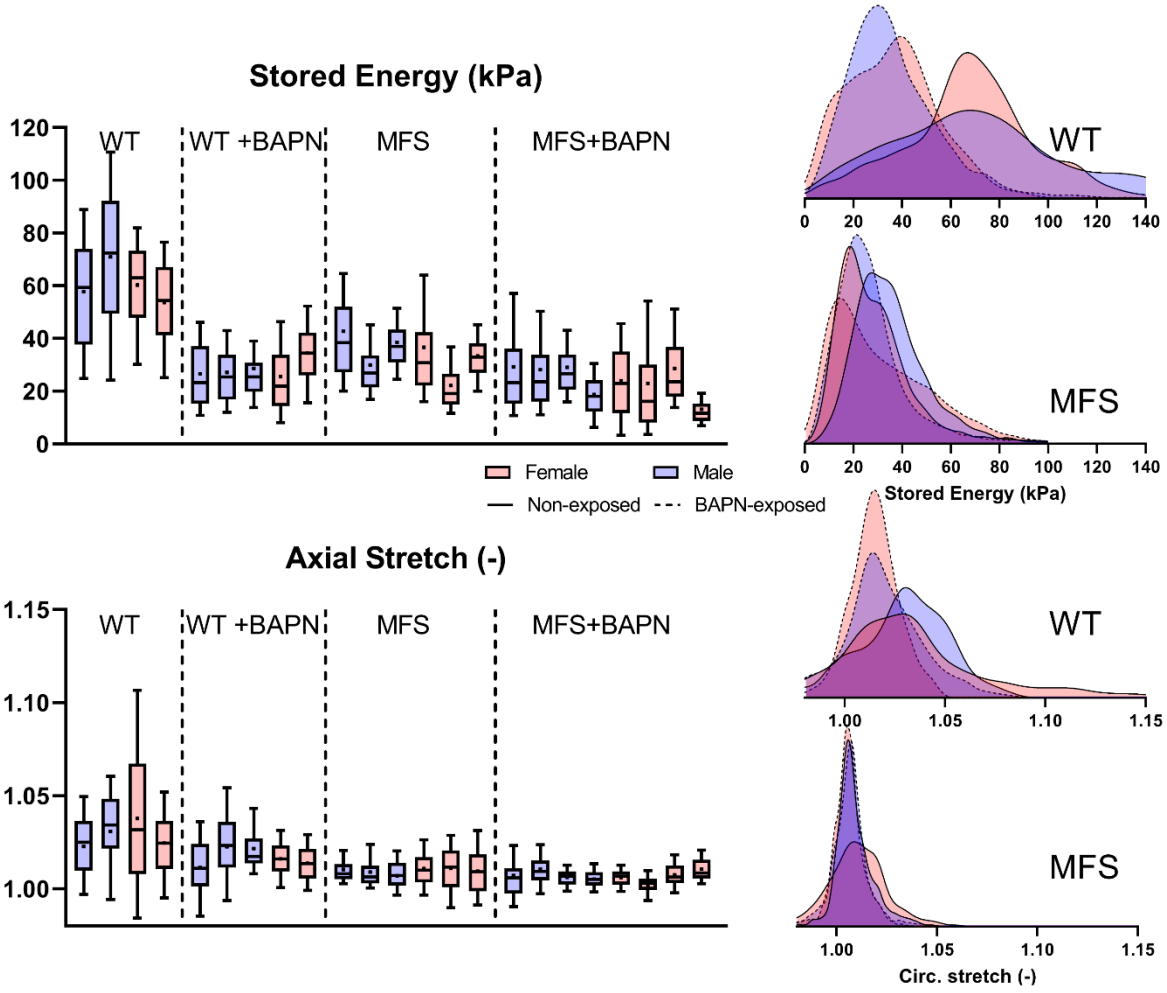

Figure S10 - pDIC data evaluated at 8 weeks of age (4-8 week groups). Similar to Figure S9, but for elastically stored energy (top row) and (local) axial stretch (bottom row). Values were computed at 100 mmHg relative to the reference configuration (80 mmHg, and *in vivo* axial stretch). MFS, BAPN-exposed MFS, and BAPN-exposed WT mice generally had lower values of stored energy and axial stretch compared with WT mice. Each bar plot represents ~1000 results around the circumference and along the length of each specimen, thus ~23000 data points are represented in each of these plots.

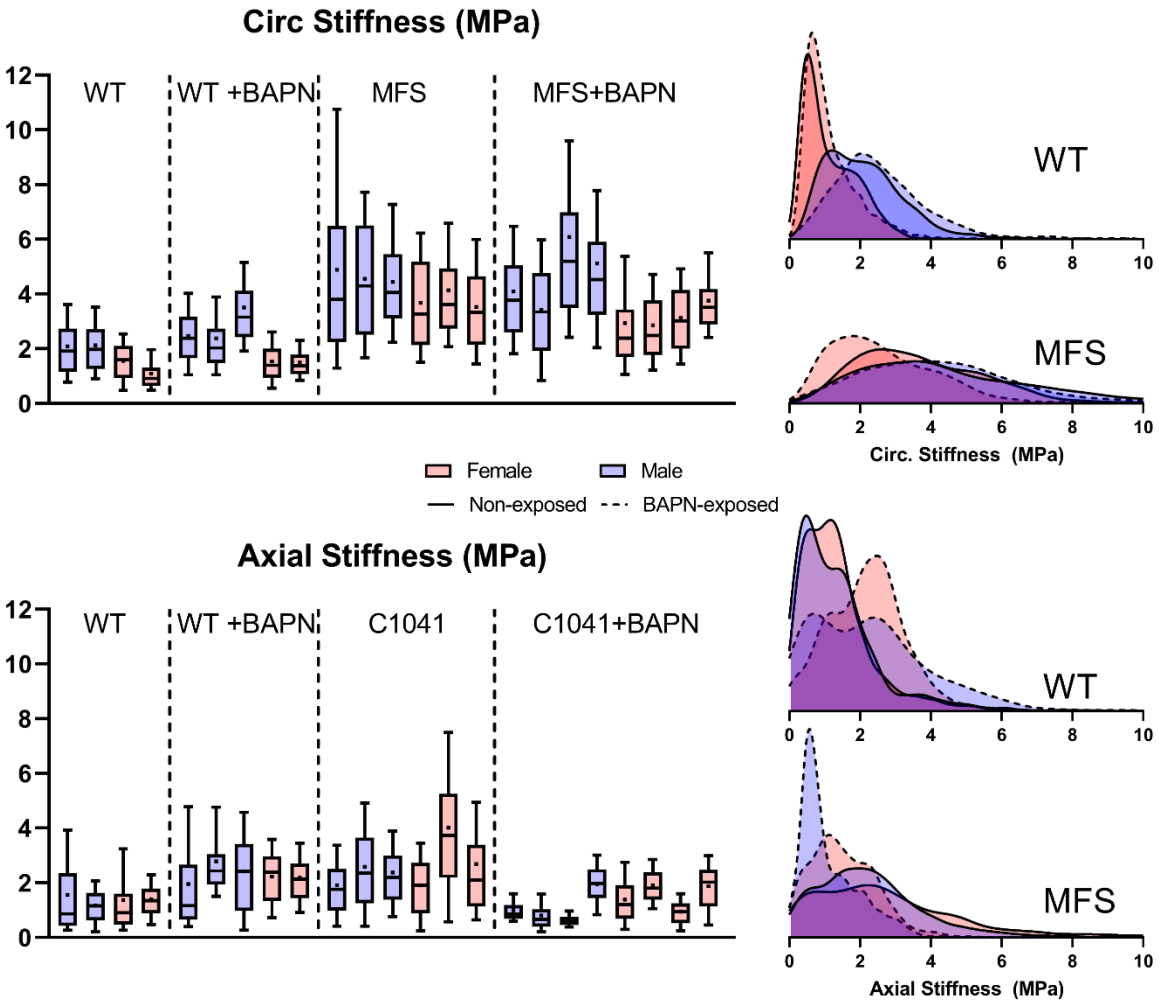

Figure S11 - pDIC data evaluated at 8 weeks of age (4-8 week groups). Similar to Figs S9-S10, but for specimen-specific circumferential and axial material stiffness. Values were calculated based on local material parameters identified in the inverse characterization but linearized using a theory of small deformations on large (at a common pressure of 100 mmHg and specimen-specific axial stretch). Note the increased circumferential stiffness in the Marfan groups that was not affected dramatically by BAPN. Each bar plot represents ~1000 results around the circumference and along the length of each specimen, thus ~23000 data points are represented in each of these plots.

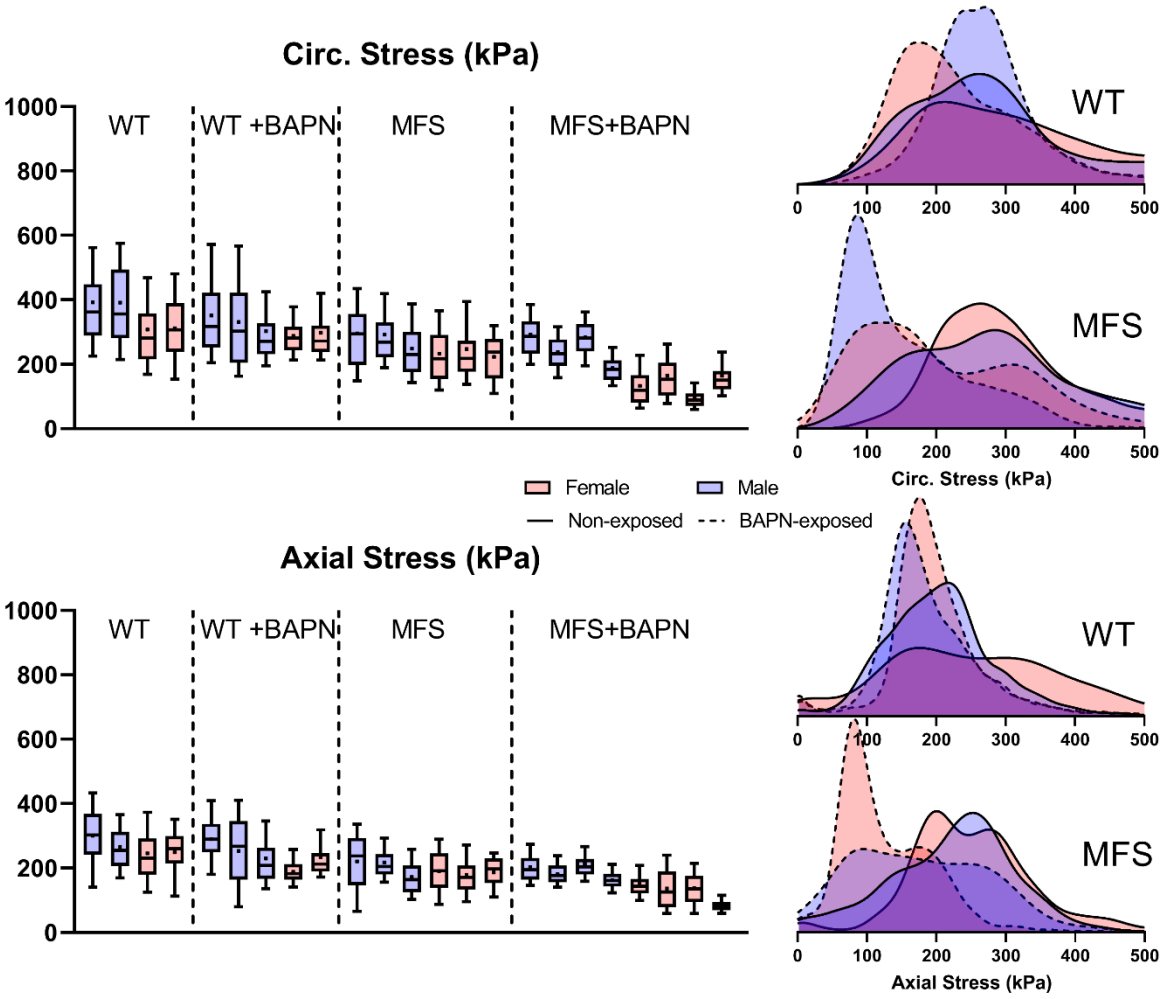

Figure S12- pDIC data evaluated at 8 weeks of age (4-8 week groups). Similar to Figs S9-S11, except for circumferential and axial Cauchy stress (kPa). Virtual field-based inverse characterization allowed these values to be computed at any state, shown here for a common pressure of 100 mmHg at the specimen-specific axial stretch. Note the general decrease in both stresses from WT to BAPN-exposed MFS. Each bar plot represents ~1000 results around the circumference and along the length of each specimen, thus ~23000 data points are represented in each of these plots.

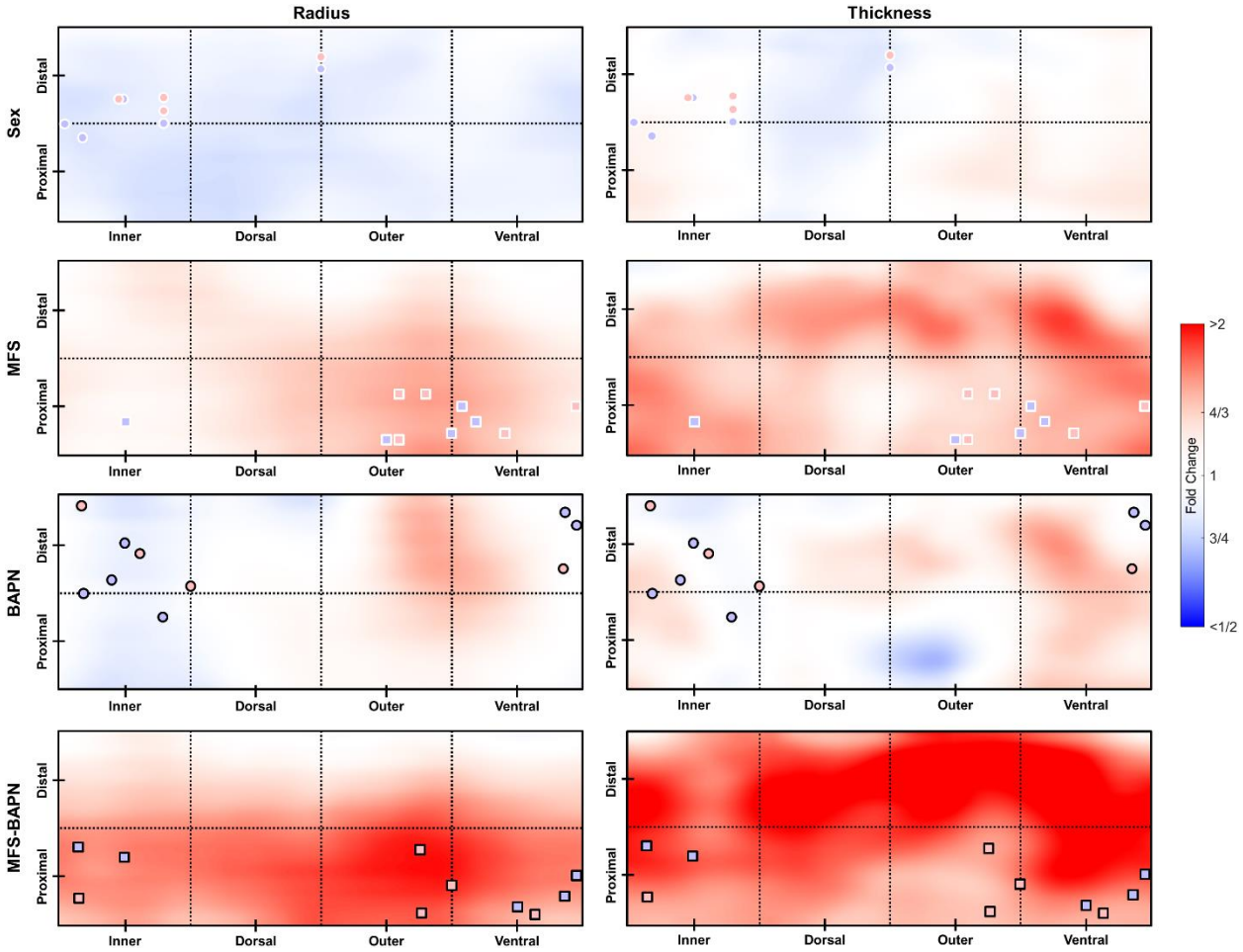

Figure S13 – Fold differences in regional luminal radius (left) and wall thickness (right) evaluated at 8 weeks of age (4-8 week groups). Maps show local fold differences as a function of sex (female relative to male), MFS (relative to WT), BAPN exposure (relative to non-exposed), and MFS + BAPN exposure (relative to non-exposed WT controls). The color axis has a logarithmic scale, such that equally substantial downward and upward fold changes are equally prominent in appearance. Plotted points indicate observed rupture sites in each group, colored and styled according to the legend in Figure 5. MFS + BAPN results are replotted here for completeness and consistency with other panels, thus allowing direct visual comparisons across these four key factors.

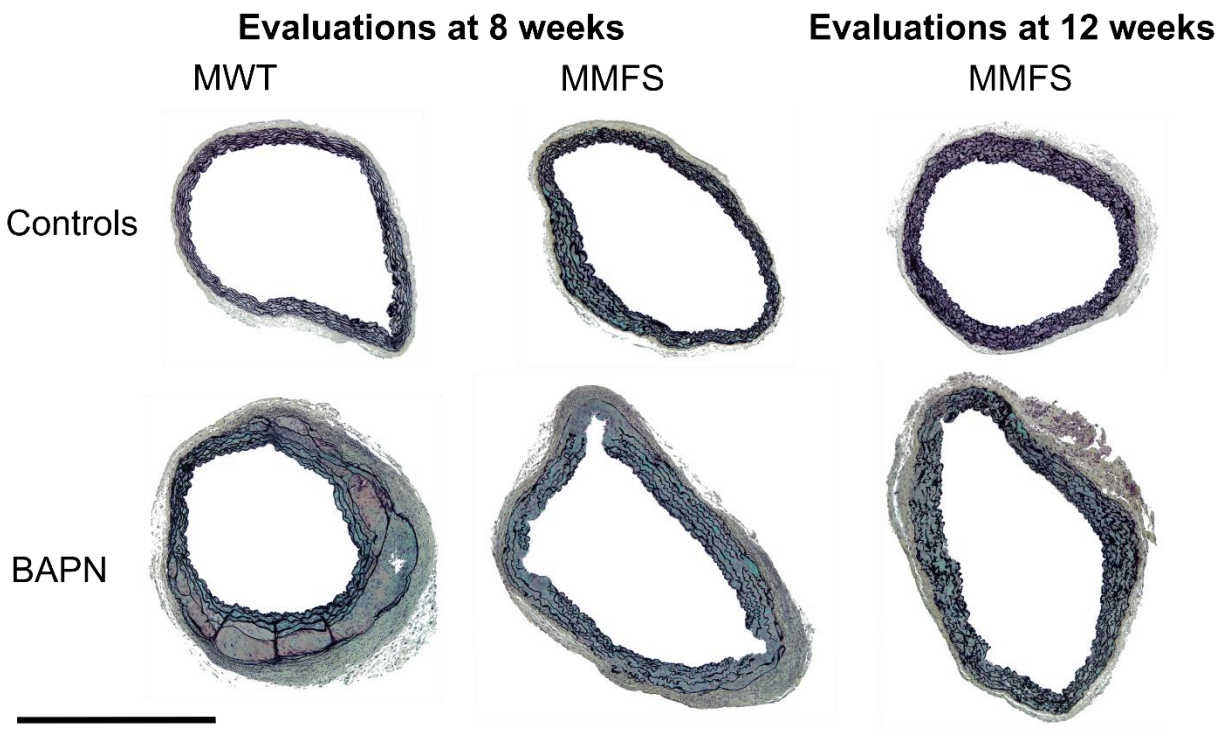

Figure S14 – Movat stained sections. Additional histological cross-sections for male (M) wild-type (WT) and *Fbn1*$^{C1041G/+}$ (MFS) mice without or with 4-week BAPN exposures starting at (left) 4 weeks of age (then evaluated at 8 weeks) or (right) 8 weeks of age (then evaluated at 12 weeks of age), with age- and sex-matched controls not receiving BAPN. These whole sections reveal spatial heterogeneities and diversity of phenotype. Note the medial delamination in the MWT aorta following early BAPN exposure (bottom, left) as well as aortic dilatation and adventitial thickening in the MMFS aorta (bottom, middle). The mucoid material (glycosaminoglycans) appeared diffuse, not pooled. Scale bar = 1 mm.

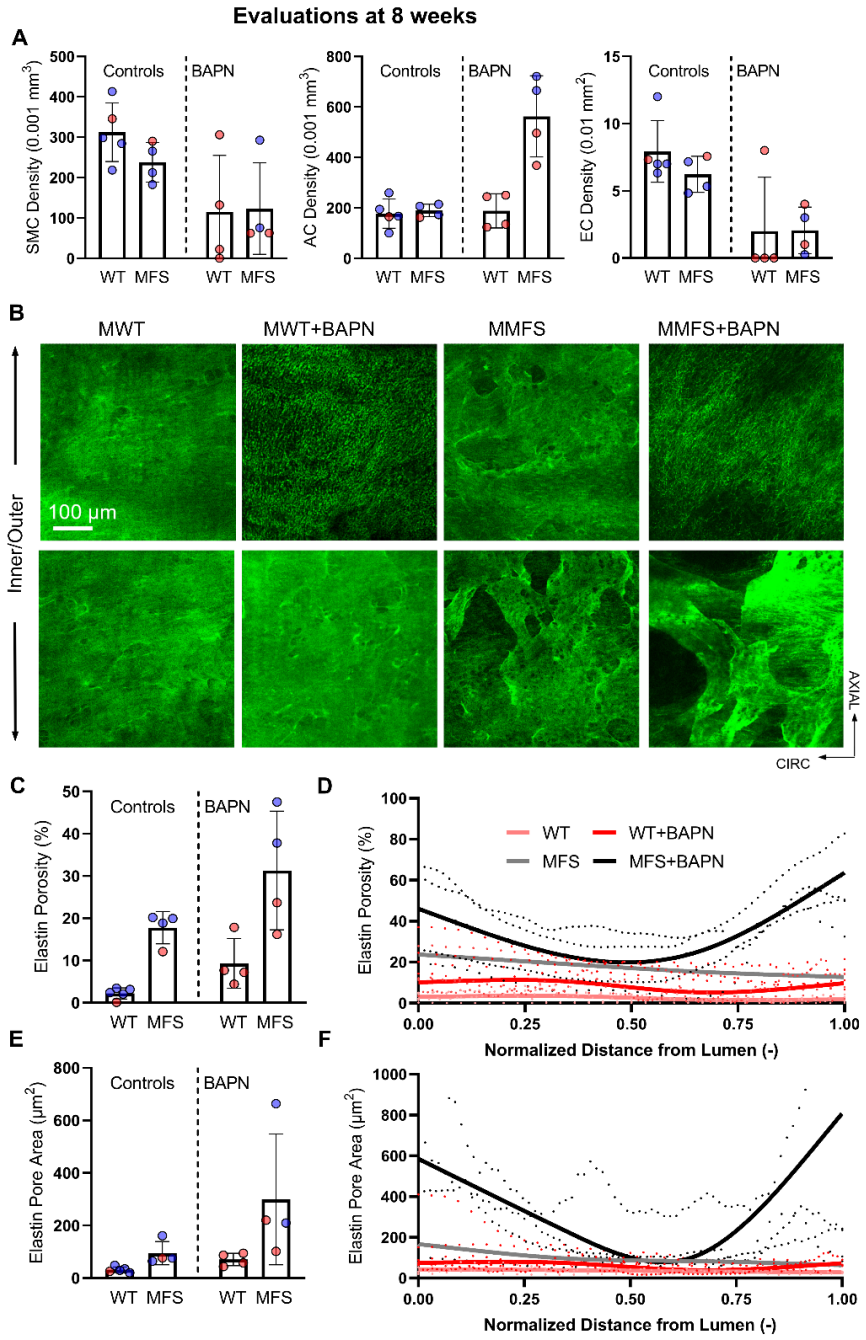

Figure S15 – Multiphoton microscopy (4-8 week groups). A. Imaging suggested in a sub-set of randomly selected vessels evaluated at 8 weeks of age (*n* = 4-5 per group, mixed sex) that there was a general decrease in endothelial and smooth muscle cell density in WT and MFS aortas following 4 weeks of BAPN exposure (i.e., from 4-8 weeks of age), but a marked increase in adventitial cell density in BAPN exposed MFS aortas, particularly in males. B-F. Two photon fluorescence (green) revealed further that elastin porosity and pore size were both initially greater in MFS than WT aortas, and these measures of compromised elastic fibers increased in MFS aortas following BAPN exposure. Importantly, the latter tended to manifest primarily in the inner and outer media, not the middle portion of the media. See **Figures 1 and S6** for detailed histological quantification based on fixed, Movat-stained cross-sections. Data are presented as means±standard deviation. No statistics were performed given the small sample size.

Major Resources Table

Genetically Modified Animals

	Species	Vendor or Source	Background Strain	Other Information	Persistent ID / URL
Parent - Male	mouse	Jackson Laboratories; strain no. 012885	*Fbn1*$^{C1041G/+}$		012885 - C1039G Strain Details (jax.org)
Parent - Female	mouse	Jackson Laboratories; strain no. 012885	*Fbn1*$^{+/+}$		012885 - C1039G Strain Details (jax.org)

Antibodies

Target antigen	Vendor or Source	Catalog #	Working concentration	Lot # (preferred but not required)	Persistent ID / URL
Recombinant Anti-LOX antibody	Abcam	ab174316	0.471 µg/ml		https://www.abcam.com/products/primary-antibodies/lox-antibody-epr4025-ab174316.html

Data & Code Availability

Description	Source / Repository	Persistent ID / URL
Histological-analysis codes	Github	https://github.com/yale-cbl/histological-analysis

Other

Description	Vendor or Source	Catalog #	Working concentration	Lot # (preferred but not required)	Persistent ID / URL
β aminopropionitrile (BAPN)	Sigma Aldrich	A3134	2 gram/liter		https://www.sigmaaldrich.com/US/en/product/sigma/a3134

ARRIVE GUIDELINES

Study Design: Please see Supplemental Figure S1 for schematic of the overall study design.

Sample Size: n=5 for passive biomechanical data previously proved sufficient for statistical comparisons and rigorous data analysis in part because of our use of highly protocolized methods and computer-control to ensure rigor and reproducibility.

Inclusion/Exclusion: Animals with severe ulcerative dermatitis and animals with terminal aortic rupture (predominantly in the male WT mice exposed to BAPN at 4 weeks of age) were excluded from the study.

Randomization: *Fbn1*$^{C1041G/+}$ mice were purchased from Jackson lab and bred in-house by a technician blinded to the study design. Mice were labeled using toe clips before tail snip taken for genotyping and then randomly assigned to a cage (up to 5 mice per cage), only separated by sex. Cages were randomly provided with either normal or BAPN- added water.

Blinding: Not available